# Supplementary Information

## HOXB13 suppresses *de novo* lipogenesis through HDAC3-mediated epigenetic reprogramming in prostate cancer

Xiaodong Lu[1], Ka-wing Fong[1], Galina Gritsina[1], Fang Wang[1], Sylvan C. Baca[2], Lourdes T. Brea[1], Jacob E. Berchuck[2], Sandor Spisak[2], Jenny Ross[3], Colm Morrissey[7], Eva Corey[7], Navdeep S. Chandel[4,5,9], William J. Catalona[4,6], Ximing Yang[3,4], Matthew L. Freedman[2,8], Jonathan C. Zhao[1,*], Jindan Yu[1,4,9,*]

**Supplementary Figures 1 to 7:**

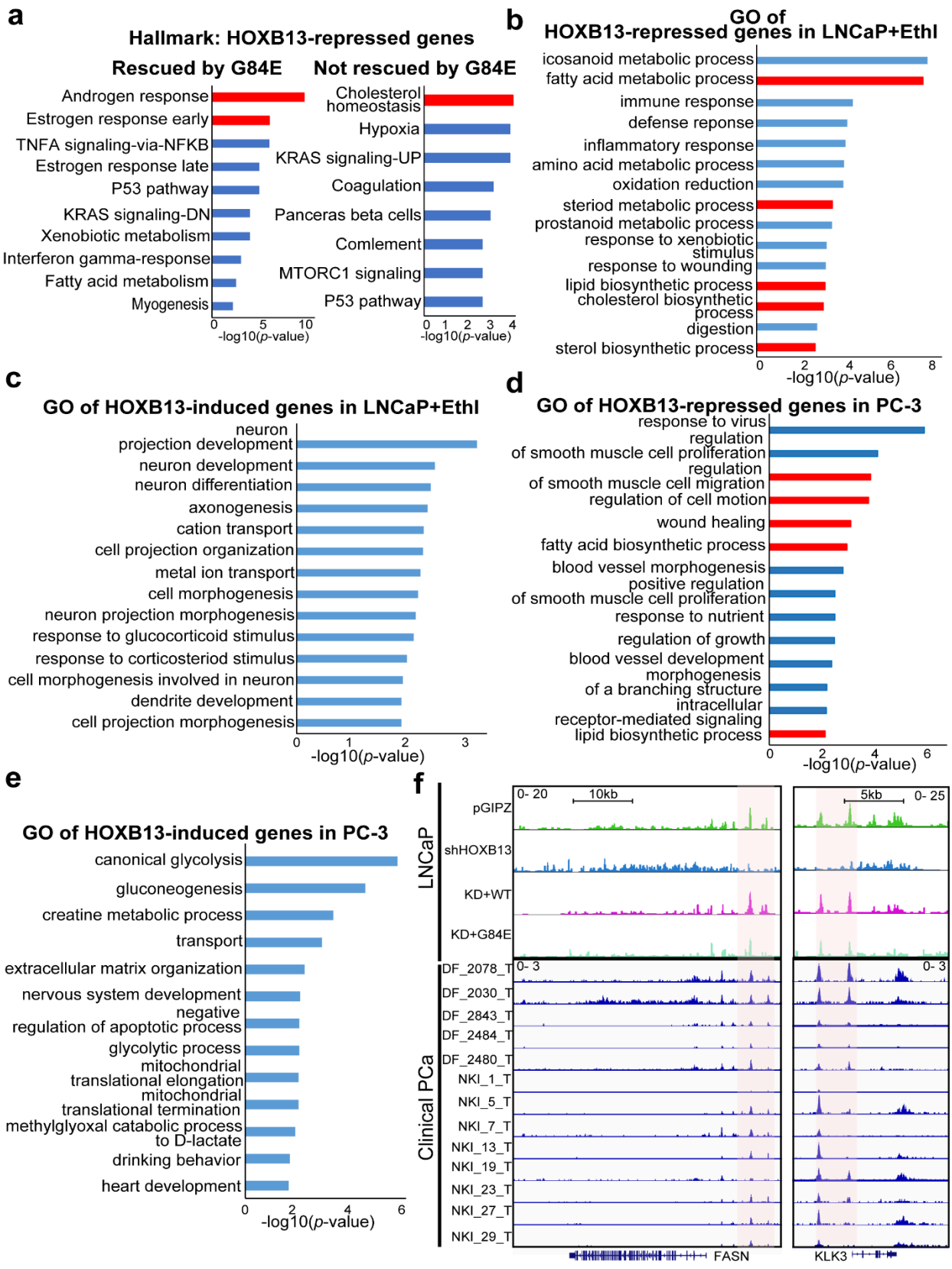
a
Hallmark: HOXB13-repressed genes
Rescued by G84E
Not rescued by G84E
Androgen response
Estrogen response early
TNFA signaling-via-NFKB
Estrogen response late
P53 pathway
KRAS signaling-DN
Xenobiotic metabolism
Interferon gamma-response
Fatty acid metabolism
Myogenesis
Cholesterol homeostasis
Hypoxia
KRAS signaling-UP
Coagulation
Panceras beta cells
Comlement
MTORC1 signaling
P53 pathway
-log10(p-value)
b
GO of HOXB13-repressed genes in LNCaP+Ethl
icosanoid metabolic process
fatty acid metabolic process
immune response
defense reponse
inflammatory response
amino acid metabolic process
oxidation reduction
steriod metabolic process
prostanoid metabolic process
response to xenobiotic stimulus
response to wounding
lipid biosynthetic process
cholesterol biosynthetic process
digestion
sterol biosynthetic process
-log10(p-value)
c
GO of HOXB13-induced genes in LNCaP+Ethl
neuron projection development
neuron development
neuron differentiation
axonogenesis
cation transport
cell projection organization
metal ion transport
cell morphogenesis
neuron projection morphogenesis
response to glucocorticoid stimulus
response to corticosteriod stimulus
cell morphogenesis involved in neuron
dendrite development
cell projection morphogenesis
-log10(p-value)
d
GO of HOXB13-repressed genes in PC-3
response to virus
regulation of smooth muscle cell proliferation
regulation of smooth muscle cell migration
regulation of cell motion
wound healing
fatty acid biosynthetic process
blood vessel morphogenesis
positive regulation of smooth muscle cell proliferation
response to nutrient
regulation of growth
blood vessel development
morphogenesis of a branching structure
intracellular receptor-mediated signaling
lipid biosynthetic process
-log10(p-value)
e
GO of HOXB13-induced genes in PC-3
canonical glycolysis
gluconeogenesis
creatine metabolic process
transport
extracellular matrix organization
nervous system development
negative regulation of apoptotic process
glycolytic process
mitochondrial translational elongation
mitochondrial translational termination
methylglyoxal catabolic process to D-lactate
drinking behavior
heart development
-log10(p-value)
f
LNCaP
pGIPZ
shHOXB13
KD+WT
KD+G84E
0- 20
10kb
5kb
0- 25
Clinical PCa
DF_2078_T
DF_2030_T
DF_2843_T
DF_2484_T
DF_2480_T
NKI_1_T
NKI_5_T
NKI_7_T
NKI_13_T
NKI_19_T
NKI_23_T
NKI_27_T
NKI_29_T
0- 3
0- 3
FASN
KLK3

**Supplementary Fig.1. Genome-wide analysis revealed an essential molecular function of HOXB13 in suppressing *de novo* lipogenesis.**

**a**. Hallmark analysis of HOXB13-repressed genes that are rescued by G84E (**left**) and not rescued by G84E (**right**) identified in Fig.1a (**Supplementary Table 3**). Top enriched molecular concepts are shown. The X-axis indicates enrichment significance. *P* values was calculated by the hypergeometric test.

**b-c**. GO analysis of HOXB13-repressed (**b**) and -induced genes (**c**) in hormone-deprived LNCaP cells. HOXB13-induced and -repressed genes were derived by comparing control cells with HOXB13-KD cells using FDR<0.05 and fold change >2.0. Under androgen-depleted conditions, HOXB13-repressed genes remained to be strongly enriched in lipid and fatty acid metabolism, whereas HOXB13-induced genes were no longer enriched for the cell cycle.

**d-e**. GO analysis of HOXB13-repressed (**d**) and -induced genes (**e**) in AR-negative PC-3 cells. PC-3 cells were subjected to control or shHOXB13 for seven days and then harvested for RNA-seq in replicate experiments. HOXB13-repressed and -induced genes were derived by comparing control cells with HOXB13-KD cells using FDR<0.05 and fold change >=2.0. HOXB13-repressed genes continued to strongly enrich for lipid and fatty acid metabolism, whereas HOXB13-induced genes were not involved in concepts related to cell proliferation.

**f.** Genome browser tracks showing HOXB13 occupancy at representative enhancers (pink shaded areas) in LNCaP, which overlaps with HOXB13 occupancy in clinical PCa, shown by IGV. KLK3, chr19:51,358,171-51,364,020 and FASN, chr17:80,036,214-80,056,106 on hg19.

GO analyses in **b-e** were performed by DAVID, top enriched molecular concepts are shown. The X-axis indicates enrichment significance, one-sided Fisher's Exact Test was performed, and -log10 (*p*-values) are shown.

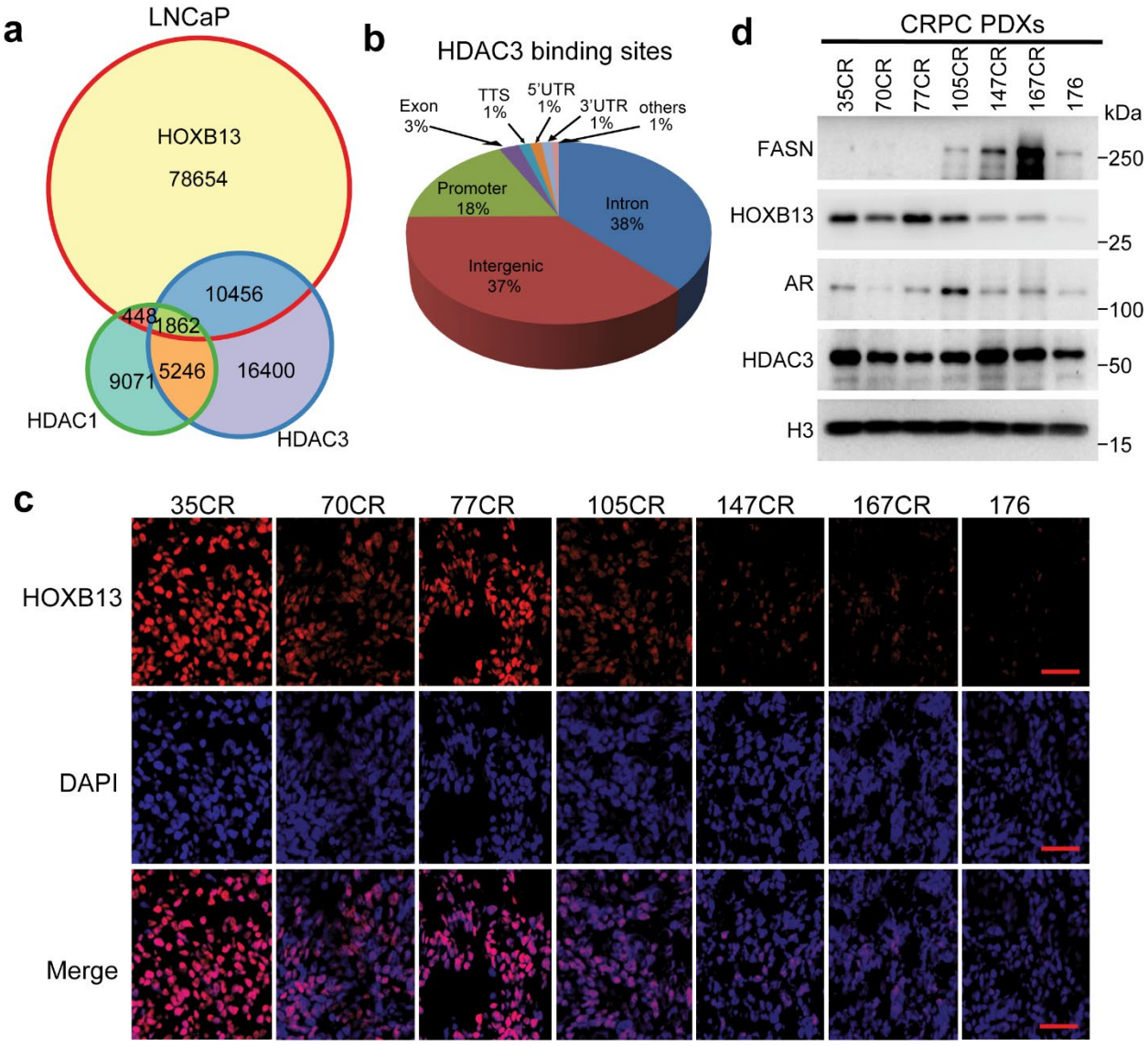


**Supplementary Fig.2. HOXB13 recruits HDAC3 to catalyze histone deacetylation.**
**a**. Venn diagram showing overlap of HOXB13, HDAC1, and HDAC3 binding sites in LNCaP. There was much more overlap between the binding sites of HOXB13 and HDAC3 than HOXB13 and HDAC1.
**b**. Pie chart showing the genomic distribution of HDAC3 binding sites in LNCaP cells. Like HOXB13, HDAC3 preferential binds to intronic and intergenic enhancers, while HDAC1 was previously shown to occupy more at gene promoters[1].
**c**. Immunofluorescence showing HOXB13 staining in 7 CRPC PDXs. Representative images of HOXB13 staining are shown. Scale bar, 20 μm. DAPI staining marks nuclei.
**d**. WB analysis of the expression of HOXB13, FASN, AR, and HDAC3 in 7 CRPC PDXs, including HOXB13-high (35CR, 70 CR, 77CR, and 105CR) and HOXB13–low PDXs (147CR, 167CR, and 176).

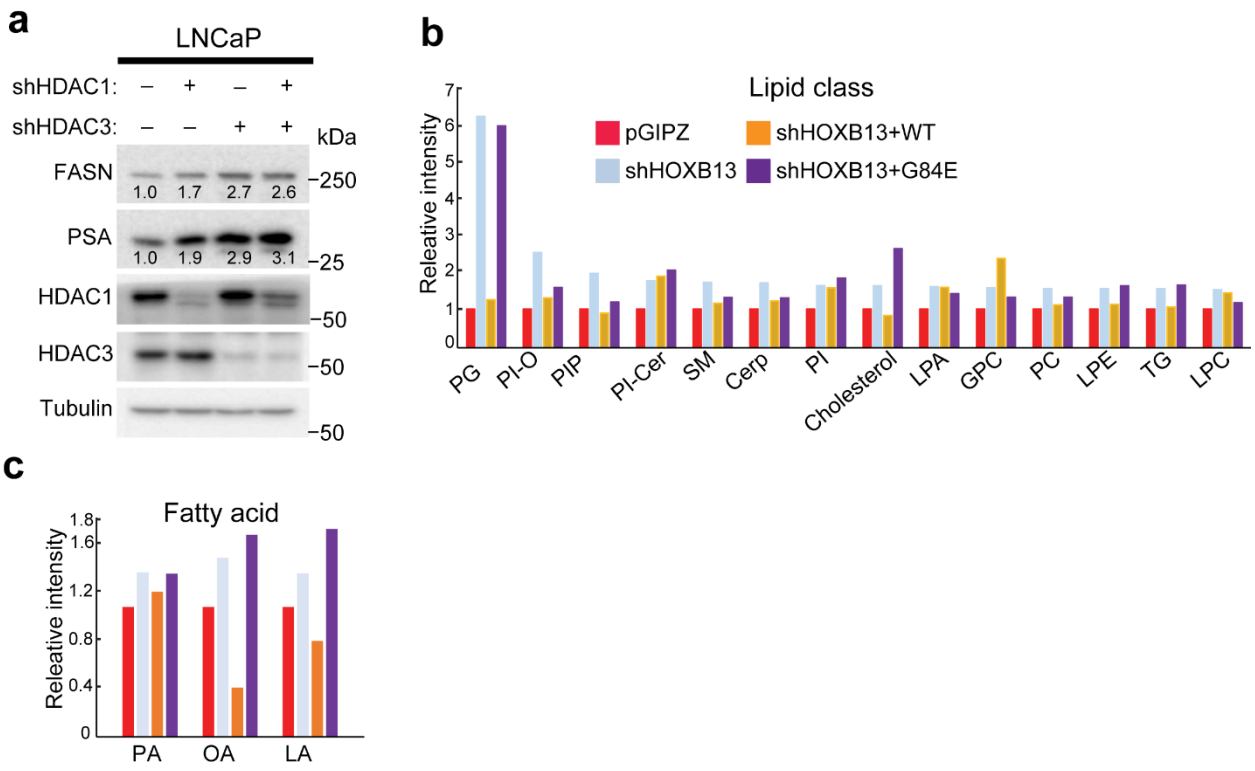


**Supplementary Fig.3. HOXB13 represses *de novo* lipogenesis.**
**a**.WB analysis of FASN and PSA in LNCaP cells with KD of HDAC1, HDAC3, or both. Whole-cell lysates from cells with indicated knockdown were analyzed by WB using anti-FASN, anti-PSA, anti-HDAC1, and anti-HDAC3 antibodies. Tubulin was used as a loading control. Quantification of FASN and PSA using BioRad Image Lab 6.
**b**. Untargeted lipidomics analysis of LNCaP cells with HOXB13 de-regulation showed that most of the lipids were increased following HOXB13 KD and rescued by the re-expression of WT, but not G84E mutant. Lipids were extracted using the Folch method, and the extracted lipids were subjected to untargeted lipidomics analysis by Q-TOF LC/MS. The top 14 HOXB13-repressed lipid classes (left) are shown. PG, Glycerophosphoglycerols; PI-O, 1-alkyl,2-acylglycerophosphoinositols; PIP, Glycerophosphoinositol monophosphates; PI-Cer, Ceramide phosphoinositols; SM, Sphingomyelins; Cerp, Ceramide 1-phosphates; PI, Glycerophosphoinositols; Cholesterol; LPA, lysoglycerophosphates; GPC, Glycanglycerophosphocholines; PC, Glycerophosphocholines; LPE, lysophosphatidylethanolamine; TG, Triradylglycerolipids; LPC, lysoglycerophosphocholines.
**c.** HOXB13-repressed fatty acid, PA: Palmitic acid; OA: Oleic acid; LA: Linoleic acid.

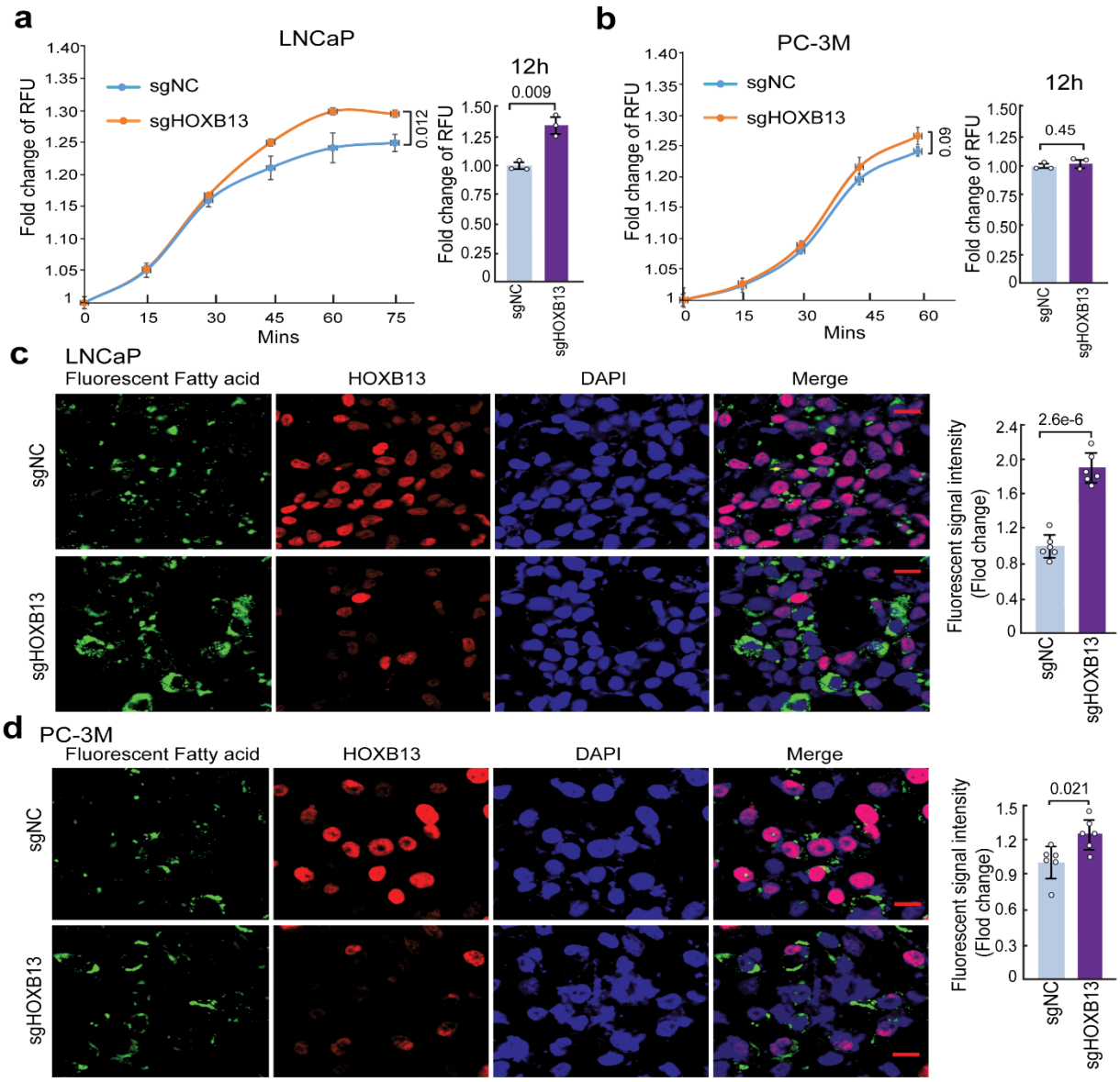


**Supplementary Fig.4. Fatty acid uptake is slightly increased in PCa cells by HOXB13 knockdown.**

**a-b.** Kinetics of fatty acid uptake by control (sgNC) or HOXB13-KD (sgHOXB13) LNCaP (**a**) and PC-3M (**b**) cells. Data shown are fluorescence intensity (**RFU**) normalized to 0 min time point over a short (0-75mins) (**left**) and long (12h) (**right**) time course after the addition of fluorescence-labeled fatty acids. Data shown are the mean ±s.d of technical replicates from one of two (n=2) independent experiments. *P* values were calculated by unpaired two-sided *t*-test. **c-d**. Confocal imaging showing increased fluorescent fatty acid uptake in HOXB13-KD (sgHOXB13) LNCaP (**c**) and PC-3M (**d**) 12h after fluorescent fatty acid addition. Scale bar: 10 µm. Fluorescent signal intensity was quantified and normalized to sgNC non-target control (**right**). Each data point represents an average of 6 (n=6) fields per independent experiment by image J. Data are the mean ±s.d. *P* values are by unpaired two-sided *t*-tests. HOXB13 loss induced the expression of several genes involved in fatty acid uptake (**Supplementary Table 4**).

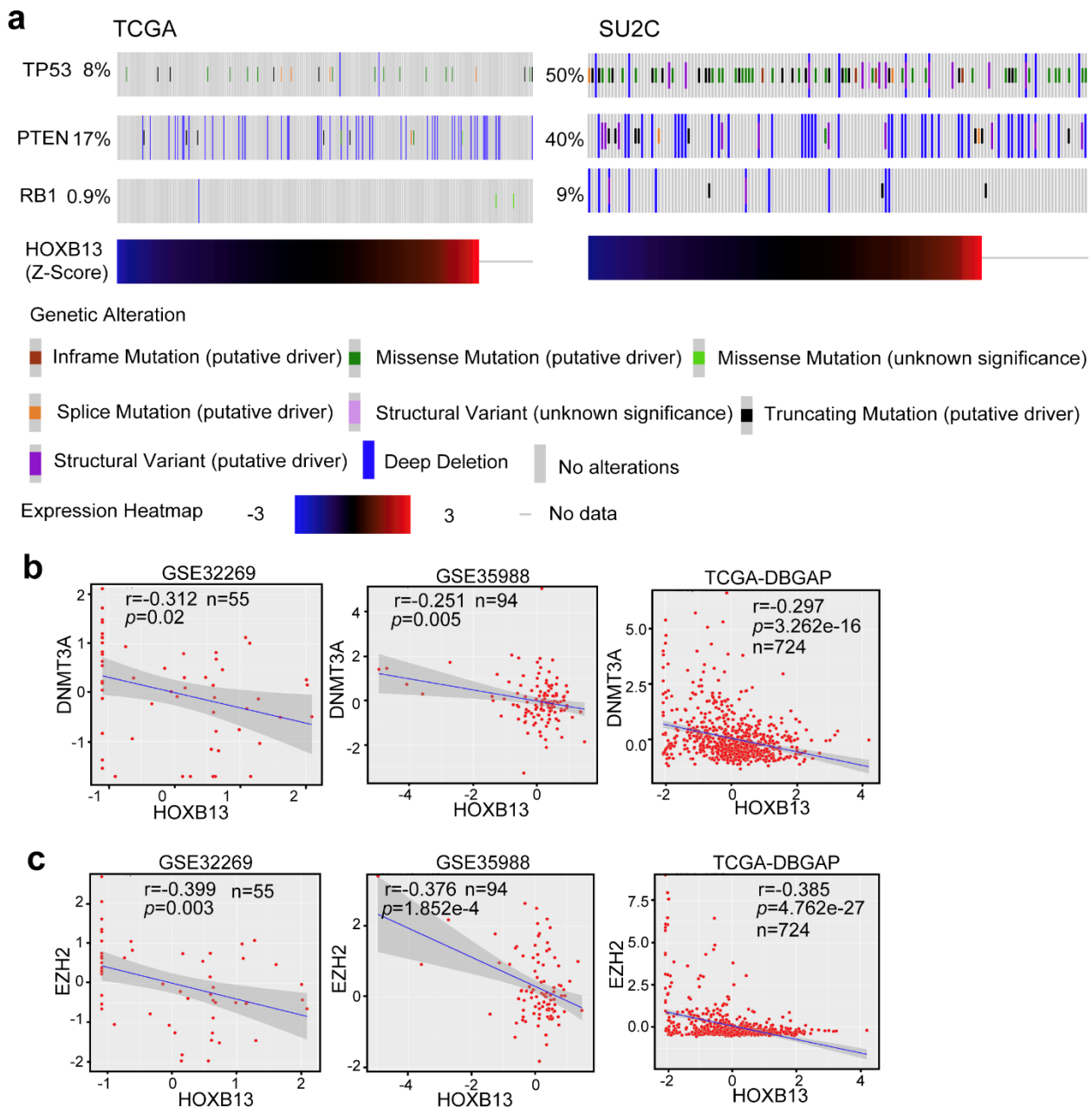


**Supplementary Fig.5. HOXB13 expression is not associated with TP53, PTEN, and RB1 status but is negatively correlated with DNMT3A and EZH2 levels in human PCa.**
**a.** Analysis of HOXB13 mRNA expression (Z-Score) and genetic alteration status of PTEN, TP53, and RB1 in TCGA and SU2C datasets available in cBioportal.
**b-c**. Negative correlation between the mRNA of HOXB13 and DNMT3A (**b**) or EZH2 (**c**) in multiple publicly available PCa datasets. Shown at X and Y axis in GSE32269 are Z-scores of log2(MAS5.0 signal intensity+1), in GSE35988 are Z-scores of log2( ratio of test/reference), and in the TCGA-dbGaP are Z-scores of log2(FPKM). The TCGA-dbGaP dataset combines prostate samples from dbGaP datasets with accession#: phs000178 (TCGA), phs000443, phs000915, and phs000909. The linear regression line (blue) with its 95% confidence interval (gray) is shown.

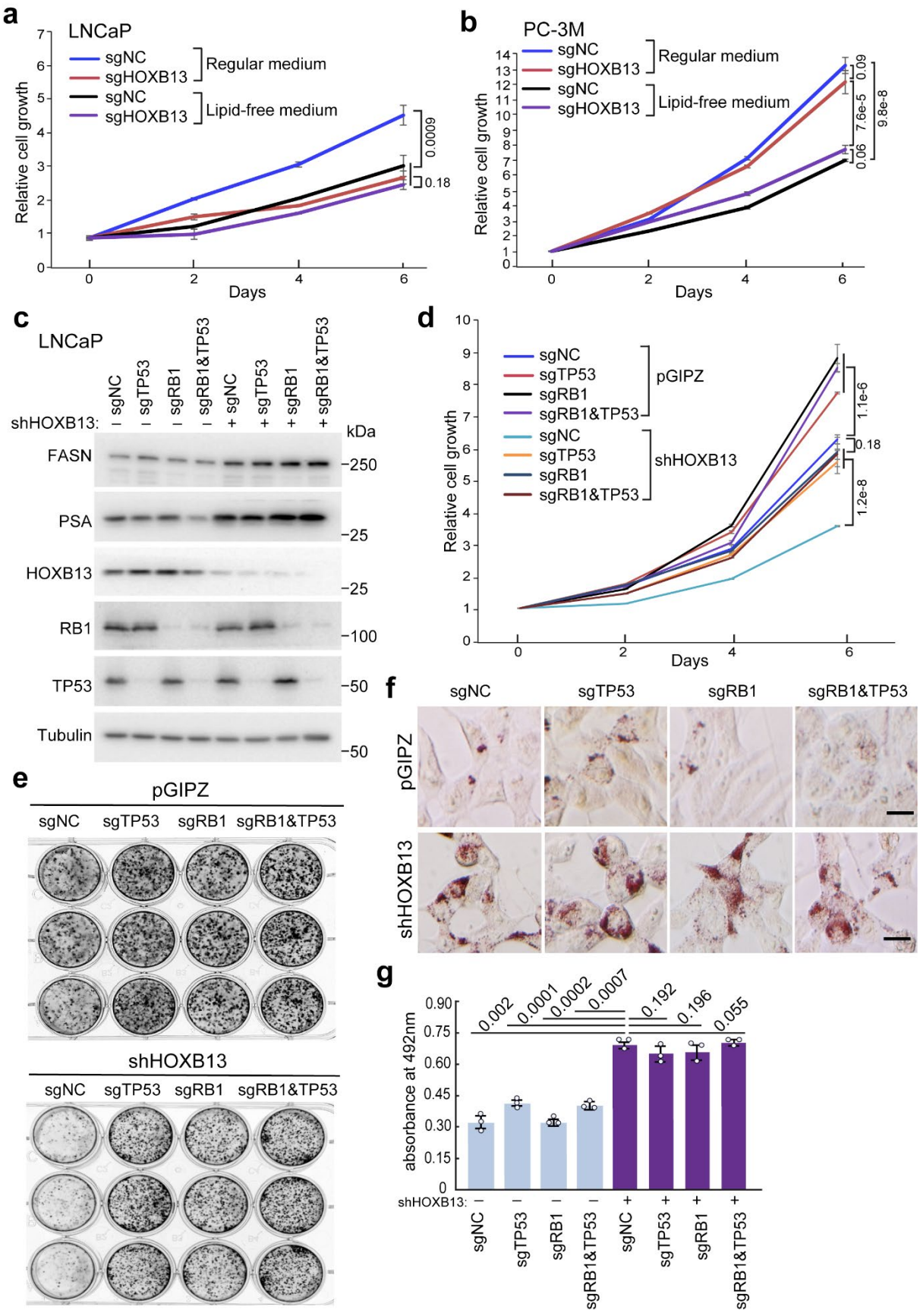
a
LNCaP
sgNC
sgHOXB13
Regular medium
sgNC
sgHOXB13
Lipid-free medium
Relative cell growth
Days
0.0009
0.18
b
PC-3M
sgNC
sgHOXB13
Regular medium
sgNC
sgHOXB13
Lipid-free medium
Relative cell growth
Days
0.09
7.6e-5
9.8e-8
0.06
c
LNCaP
shHOXB13:
sgNC
sgTP53
sgRB1
sgRB1&TP53
sgNC
sgTP53
sgRB1
sgRB1&TP53
kDa
FASN
PSA
HOXB13
RB1
TP53
Tubulin
250
25
25
100
50
50
d
sgNC
sgTP53
sgRB1
sgRB1&TP53
pGIPZ
sgNC
sgTP53
sgRB1
sgRB1&TP53
shHOXB13
Relative cell growth
Days
1.1e-6
0.18
1.2e-8
e
pGIPZ
sgNC
sgTP53
sgRB1
sgRB1&TP53
shHOXB13
sgNC
sgTP53
sgRB1
sgRB1&TP53
f
sgNC
sgTP53
sgRB1
sgRB1&TP53
pGIPZ
shHOXB13
g
absorbance at 492nm
0.002
0.0001
0.0002
0.0007
0.192
0.196
0.055
shHOXB13:
sgNC
sgTP53
sgRB1
sgRB1&TP53
sgNC
sgTP53
sgRB1
sgRB1&TP53

**Supplementary Fig.6. HOXB13 loss induced lipid accumulation independent of RB1 and TP53 genomic alteration.**

**a-b.** WST-1 assay of cell proliferation in control (sgNC) or HOXB13 KD (sgHOXB13) LNCaP cells and PC-3M cells cultured in lipid-free or regular medium (10% FBS). Lipid starvation using lipid-free medium reduced control LNCaP cell growth but did not affect HOXB13-KD cells, likely due to these cells already in cell cycle arrest.

**c**. WB analysis of FASN, PSA, HOXB13, TP53, and RB1 in control or HOXB13-KD LNCaP cells on control (sgNC), TP53 or RB1 single or double knockout background.

**d-e**. WST-1 cell proliferation (**d**) and colony formation (**e)** assays of LNCaP cells as shown in **c**. Depletion of key cell cycle suppressors TP53 and/or RB1 rescued HOXB13-KD cell proliferation and further increased control (pGIPZ) cell growth.

**f-g**. Oil Red O staining and quantification of lipid accumulation in LNCaP cells with indicated gene de-regulation. Data (**f**) shown are representative Oil Red O staining images with a Scale bar of 30 μm. The stain was extracted in isopropanol and quantified at 492 nm (**g**). Data shown are mean ± s.d of triplicate wells from one of two (n=2) independent experiments. Unpaired two-sided *t*-test was performed between indicated groups as shown in figures. Loss of HOXB13 increased lipid accumulation irrespective of TP53 and RB1 status

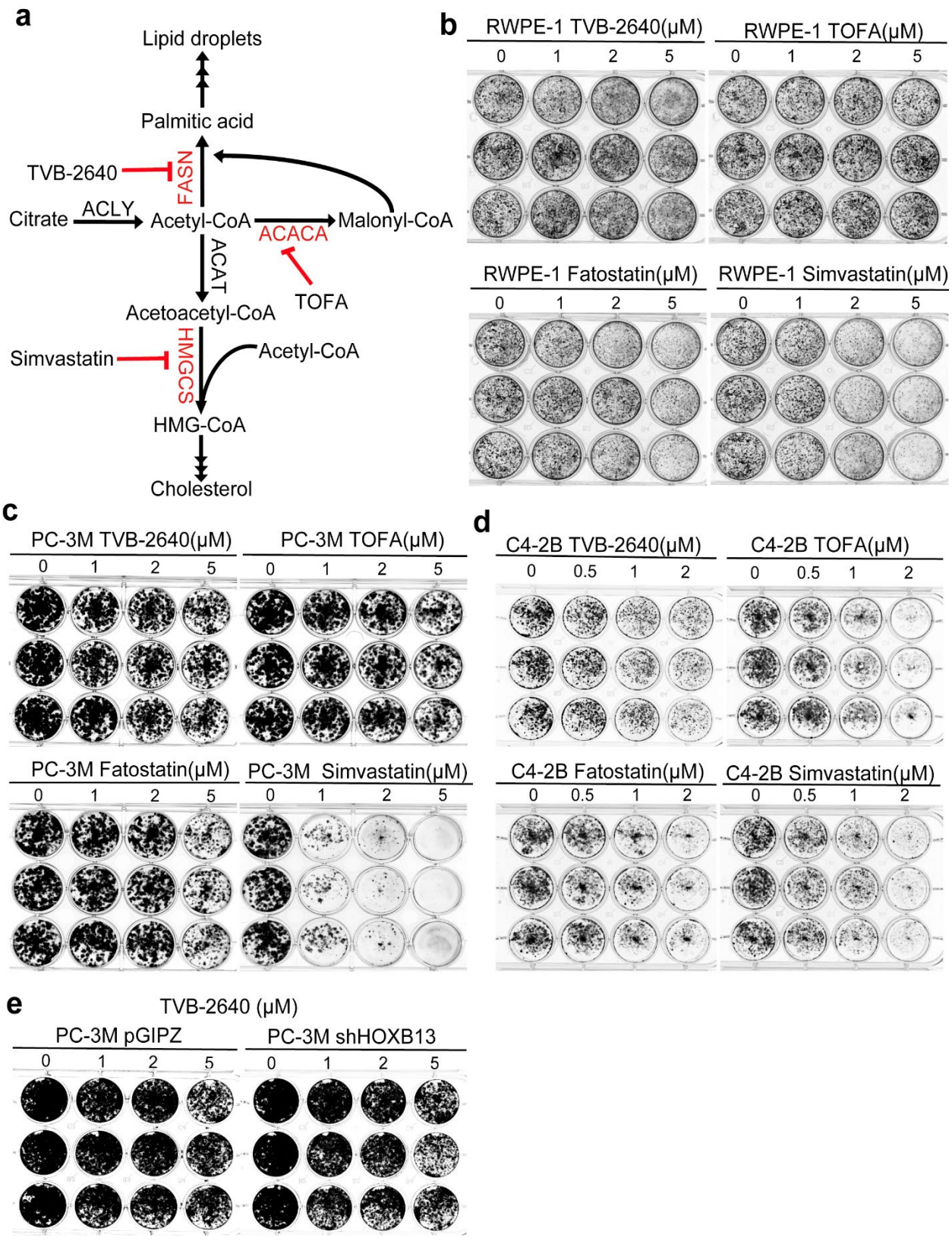
a
Lipid droplets
Palmitic acid
TVB-2640
FASN
Citrate
ACLY
Acetyl-CoA
Malonyl-CoA
ACACA
ACAT
TOFA
Acetoacetyl-CoA
Simvastatin
HMGCS
Acetyl-CoA
HMG-CoA
Cholesterol
b
RWPE-1 TVB-2640(μM)
0 1 2 5
RWPE-1 TOFA(μM)
0 1 2 5
RWPE-1 Fatostatin(μM)
0 1 2 5
RWPE-1 Simvastatin(μM)
0 1 2 5
c
PC-3M TVB-2640(μM)
0 1 2 5
PC-3M TOFA(μM)
0 1 2 5
PC-3M Fatostatin(μM)
0 1 2 5
PC-3M Simvastatin(μM)
0 1 2 5
d
C4-2B TVB-2640(μM)
0 0.5 1 2
C4-2B TOFA(μM)
0 0.5 1 2
C4-2B Fatostatin(μM)
0 0.5 1 2
C4-2B Simvastatin(μM)
0 0.5 1 2
e
TVB-2640 (μM)
PC-3M pGIPZ
0 1 2 5
PC-3M shHOXB13
0 1 2 5

**Supplementary Fig.7. Effects of various lipogenic inhibitors on normal prostate and PCa cell growth.**

**a**. Schematic overview of lipid synthesis, cholesterol synthesis pathway. The key genes involved in *de novo* lipogenesis and cholesterol synthesis are shown, and the genes highlighted in red are upregulated in HOXB13-KD cells (details in **Supplementary Table 5**). FASN inhibitor: TVB-2640; ACACA inhibitor: TOFA; HMGCS inhibitor: Simvastatin.

**b-d**. Colony formation assays of normal prostate epithelial cell line RWPE-1, AR-positive PCa cell line C4-2B, and AR-negative PCa cell line PC-3M treated with different lipogenesis inhibitors, as shown in **a,** at indicated doses. Simvastatin at >1μM and Fatostatin (SREBF1/2 inhibitor) at >2μM reduced RWPE-1 cell growth, indicating cytotoxicity. By contrast, TVB-2640 and TOFA were well tolerated by RWPE-1 cells but specifically reduced C4-2B, and to a lesser extent, PC-3M PCa cell growth, with TVB-2640 showing better anti-growth effects than TOFA.

**e**. Colony formation assays were performed in control and HOXB13-KD PC-3M cells treated with TVB-2640. TVB-2640 showed similar efficacy in reducing the growth of HOXB13-KD as control PC-3M cells.

**Reference**:

1. Chng, K.R. *et al.* A transcriptional repressor co-regulatory network governing androgen response in prostate cancers. *EMBO J* **31**, 2810-23 (2012).

Supplementary Fig.2d

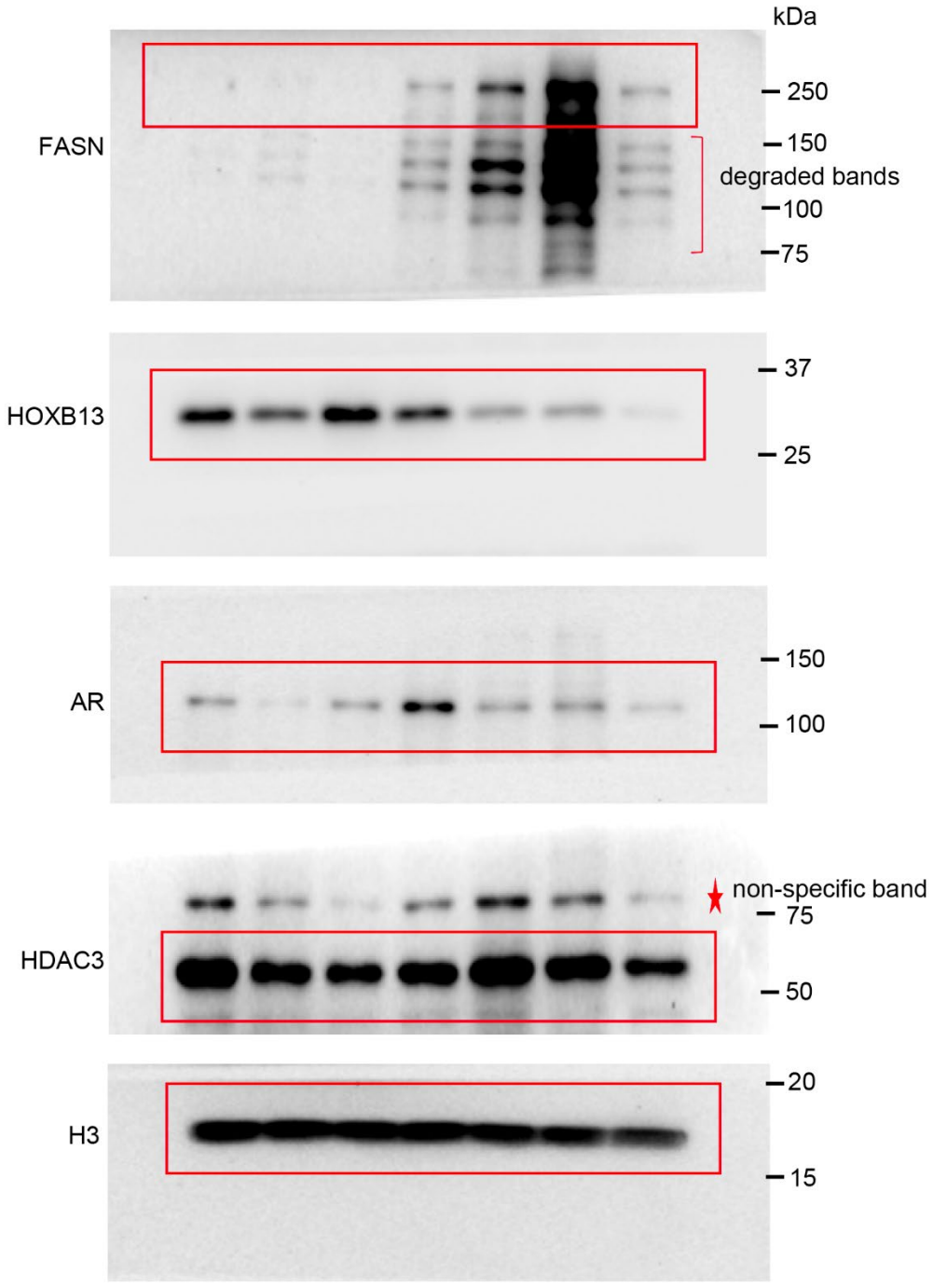

Supplementary Fig.3a

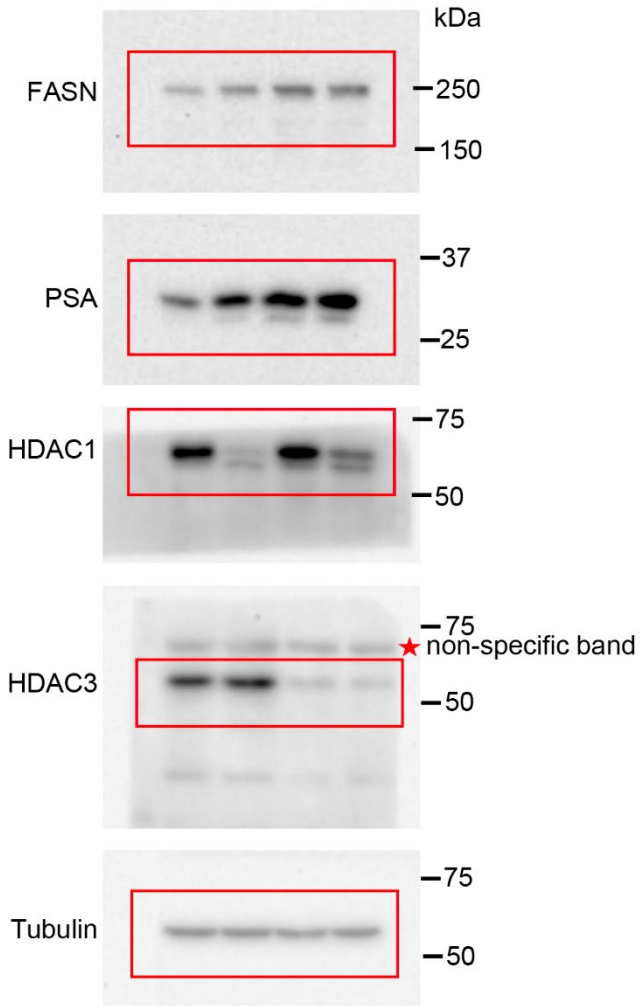

Supplementary Fig.6c